Scientia Pharmaceutica

ÖSTERREICHISCHE PHARMAZEUTISCHE GESELLSCHAFT

MDPI

Article

Purified Clinoptilolite-Tuff as a Trap for Amines Associated with Chronic Wounds: Binding of Cadaverine, Putrescine, Histamines and Polyamines

Ali El-Kasaby [1], Christian Nanoff [1], Stephane Nizet [2], Cornelius Tschegg [2] and Michael Freissmuth [1,*]

[1] Institute of Pharmacology and the Gaston H. Glock Research Laboratories for Exploratory Drug Development, Centre of Physiology and Pharmacology, Medical University of Vienna, Währinger Str. 13A, 1090 Vienna, Austria; ali.elkasaby@meduniwien.ac.at (A.E.-K.); christian.nanoff@meduniwien.ac.at (C.N.)

[2] GLOCK Health, Science and Research GmbH, Hausfeldstrasse 17, 2232 Deutsch-Wagram, Austria; stephane.nizet@glock.at (S.N.); cornelius.tschegg@glock.at (C.T.)

* Correspondence: michael.freissmuth@meduniwien.ac.at; Tel.: +43-1-4016031371

Abstract: Ulcerous lesions can arise in primary skin cancers and upon infiltration of the skin by malignant cells originating from other organs. These malignant fungating wounds are difficult to treat, and they cause pain, itching and malodor. Distressing malodor imposes a major burden on patients. The carrion odor of decaying tissue is—at least in part—due to the bacterial breakdown products cadaverine and putrescine. Here, we examined the binding of cadaverine, histamine, putrescine, spermidine and spermine to the preparation of micronized purified clinoptilolite-tuff (PCT) by relying on three radiolabeled tracers ([^{3}H]cadaverine, [^{3}H]histamine and [^{3}H]spermidine). Binding was rapid, stable and of high capacity. The binding affinities were in the low μM range. Displacement experiments indicated that the binding sites were non-equivalent. These three properties combined to support effective binding for any given ligand in the presence of the expected, submillimolar concentrations of competing ligands. This was further verified by measuring the binding of [^{3}H]cadaverine in the presence of wound drainage fluids. [^{3}H]Cadaverine was effectively adsorbed by a wound dressing, into which purified clinoptilolite-tuff had been incorporated: the observed binding capacity of this wound dressing was consistent with its content of purified clinoptilolite-tuff. Based on these findings, we propose that purified clinoptilolite-tuff be further investigated as a means to control malodor emanating from chronic wounds.

Keywords: purified clinoptilolite-tuff; fungating wounds; cadaverine; histamine; putrescine; spermidine; spermine

Academic Editor: Roman B. Lesyk

Received: 21 November 2024
Revised: 17 January 2025
Accepted: 21 January 2025
Published: 23 January 2025

Citation: El-Kasaby, A.; Nanoff, C.; Nizet, S.; Tschegg, C.; Freissmuth, M. Purified Clinoptilolite-Tuff as a Trap for Amines Associated with Chronic Wounds: Binding of Cadaverine, Putrescine, Histamines and Polyamines. *Sci. Pharm.* **2025**, *93*, 7. https://doi.org/10.3390/scipharm93010007

1. Introduction

Solid cancers arising in internal organs metastasize primarily to lymph nodes, the liver, lungs and bone [1]. Distant cutaneous metastases were originally thought to be rare, i.e., in the range of ≤1% [2,3]. However, more recent surveys suggest that skin metastases are more prevalent (up to 10%) in end-stage disease [4]. In addition, cancers, in particular of the breast, can locally infiltrate the skin. Both locally infiltrating cancers and metastases evolve into cancerous wounds, as do primary skin tumors. Necrosis and ulceration drive the formation of the wound crater, and the proliferation of the cancer cells gives rise to nodules within the wound and, thus, to the eponymous fungus-like appearance. Up to 5 to >10% of patients with advanced cancer develop fungating wounds [5,6]. Because

fungating wounds occur in terminal disease, the life expectancy of the affected patients is short and, thus, palliation of symptoms is the primary therapeutic goal.

Chronic wounds are difficult to treat. This is true, in particular, for malignant fungating wounds [7]. Tissue necrosis, exudate formation and bacterial colonization result in the accumulation of many degradation products, which give rise to malodor [6,8,9]. These include the diamines cadaverine and putrescine, which arise from the decarboxylation of lysine and ornithine, respectively [10]. The carrion smell of cadaverine and putrescine is sensed by odorant receptors of the TAAR (trace amine-associated receptor) family [11,12]; it is perceived as the smell of death, elicits a threat management response in people [13] and causes nausea and revulsion, which is not conducive to the care of patients with fungating wounds [8]. Malodor results in social isolation and is distressing to patients [14,15]. Accordingly, odor management becomes an important consideration in the management of fungating wounds. In addition, cadaverine is associated with periwound moisture-associated dermatitis, i.e., the exudate-triggered inflammation of the skin surrounding the wound [16]. Charcoal-based wound dressings are most frequently used, but sorption by charcoal is not very effective [14]. Aldehyde-functionalized cellulose was recently developed as an alternative and found to be superior to a charcoal-containing fabric in binding cadaverine [17]. However, the chemical reactivity of the aldehyde groups remains a source of concern. In addition, competing amines in the wound fluid—i.e., polyamines of bacterial origin and exudated proteins—consume the aldehyde groups. Thus, the effective binding capacity may be substantially lower than the nominal capacity. Earlier approaches to reducing malodor aimed at reducing bacterial growth by incorporating silver, iodine, metronidazole and plant-derived oils (from eucalyptus, thyme, lavender, etc.) into the wound dressing [18]. Similarly, bacterial growth may be reduced by applying hyperosmolar sucrose or manuka honey. However, the effectiveness of these approaches is considered modest in the management of malignant fungating wounds: in a systematic survey, charcoal-based dressings and metronidazole-containing gels were rated as being highly effective in about 50% of the cases. Silver- and iodine-based dressings were considered to be highly effective in only 23 and 17% of the cases, respectively; the ratings for all other approaches were even lower [14]. Thus, there is a large unmet medical need [14,18].

Clinoptilolite, a heulandite-type zeolite, is a hydrated aluminosilicate characterized by a unique framework of interconnected SiO_4 and AlO_4 tetrahedra. The negatively charged crystal framework, resulting from the isomorphous substitution of Si^{4+} by Al^{3+}, enables the mineral to absorb and exchange mono- and divalent cations within the crystal lattice [19], and to adsorb larger ions and/or molecules onto the surface [20–22]. Nizet et al. [23] and Sarabi et al. [24] recently also demonstrated that virions of various species were adsorbed to and effectively neutralized by purified clinoptilolite-tuff. Here, we explored the hypothesis that purified clinoptilolite-tuff bound diamines and polyamines with a capacity that sufficed to effectively deplete these compounds in wound exudates. The microporous structure of clinoptilolite provides a large surface area and numerous adsorption sites, and its framework harbors an overall negative net charge. Hence, it is reasonable to posit that clinoptilolite avidly interacts with the amine groups of polyamines, which—based on their pKa in the range of 9.1 to 10.8—are almost completely ionized at physiological pH [25]. We examined this hypothesis by using a preparation of micronized purified clinoptilolite-tuff (PCT), which has been shown to be well tolerated in a phase I trial with artificial wounds [26]. Our observations show that purified clinoptilolite-tuff (PCT) binds cadaverine, histamine, putrescine, spermidine and spermine with high capacity; this binding is preserved in the presence of wound fluid and is also maintained if the micronized preparation of PCT is incorporated into a wound dressing.

2. Results

2.1. Binding of [^{3}H]histamine and [^{3}H]spermidine

Many gram-positive and gram-negative bacteria express histidine decarboxylase, the enzyme required for histamine production [27], and this is also true for wound-colonizing bacteria [28]. Similarly, these bacteria express the enzymatic machinery required for the synthesis of polyamines, in particular spermidine [10]. The crystal lattice of clinoptilolite has a net negative charge, which allows for the binding of cations. Accordingly, we examined the capacity of micronized purified clinoptilolite-tuff (PCT) to adsorb radiolabeled histamine and spermidine. We first determined the time course of binding (Figure 1): Both [^{3}H]histamine and [^{3}H]spermidine bound rapidly regardless of whether they were present at concentrations in the low nanomolar range (Figure 1A,C) or at 100 μM (Figure 1B,D). The binding was stable for at least two hours.

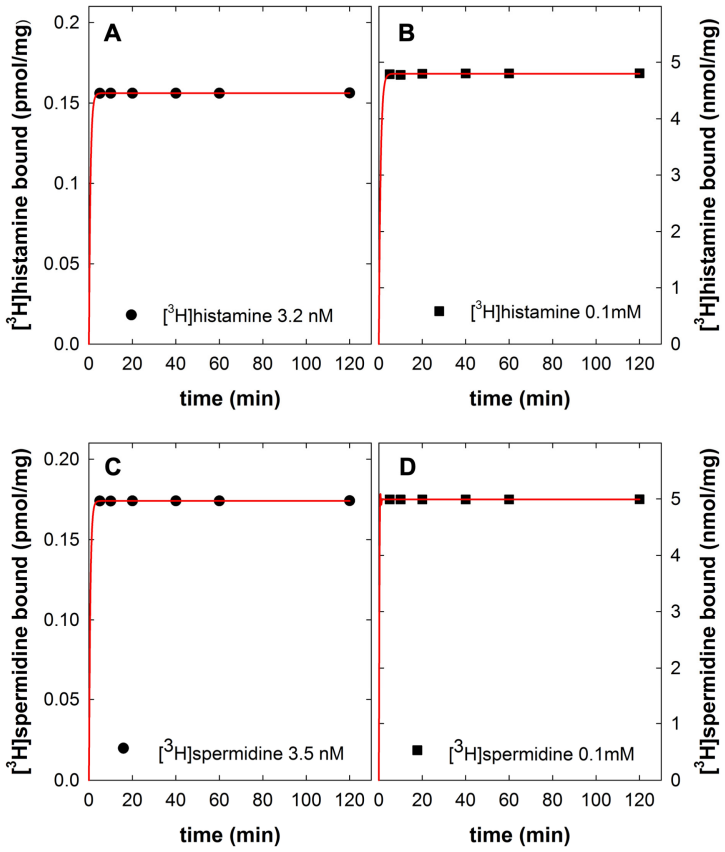

Figure 1. Time course of [^{3}H]histamine binding (**A**,**B**) and of [^{3}H]spermidine binding (**C**,**D**) to purified clinoptilolite-tuff (PCT). The binding reaction was carried out in a final volume of 0.5 mL containing PBS (phosphate-buffered saline), 10 mg PCT and either carrier-free radioligands—i.e., 3.2 nM [^{3}H]histamine (specific activity 16.4 Ci/mmol, panel **A**) and 3.5 nM [^{3}H]spermidine (specific activity 36.4 Ci/mmol, panel **C**) or [^{3}H]histamine and [^{3}H]spermidine isotopically diluted with unlabeled histamine (panel **B**,**D**) and with unlabeled histamine spermidine, respectively, to yield a concentration of 100 μM. Bound and free radioligands were separated by centrifugation, the level of free radioligand was determined by liquid scintillation and the bound amount of radioligand was calculated from the difference of total minus free as outlined in Materials and Methods. Data are from a representative experiment carried out in duplicate.

Two approaches were used to determine the binding affinity under equilibrium conditions. First, varying amounts of PCT were incubated with a fixed concentration (100 μM) of [^{3}H]histamine and [^{3}H]spermidine: half-maximum binding of [^{3}H]histamine (Figure 2A) and [^{3}H]spermidine (Figure 2B) were observed at PCT levels of 2.20 ± 0.16 mg/mL and

0.90 ± 0.03 mg/mL (means ± S.D.), respectively. Alternatively, a fixed amount of PCT (4 mg) was incubated with increasing concentrations of [^{3}H]histamine and [^{3}H]spermidine. The saturation curve for [^{3}H]histamine (Figure 2C) was adequately described by a rectangular hyperbola and thus consistent with binding to a single class of binding sites. The estimates for K_D and B_{max} extracted from the fit were 36.2 ± 15.3 µM and 43.1 ± 2.3 nmol/mg, respectively. In contrast, the binding of [^{3}H]spermidine diverged from a simple rectangular hyperbola (red curve in Figure 2D): the data points were better described by assuming the presence of two binding sites (blue curve in Figure 2D) than by a fit to a model with a single site. We estimated the following K_D and B_{max} values, $K_{D,1}$ = 1.03 ± 0.36 µM and $B_{max,1}$ = 52.9 ± 5.1 nmol/mg and $K_{D,2}$ = 2691 ± 1020 µM and $B_{max,2}$ = 100.4 ± 10.4 nmol/mg for the high- and the low-affinity sites, respectively.

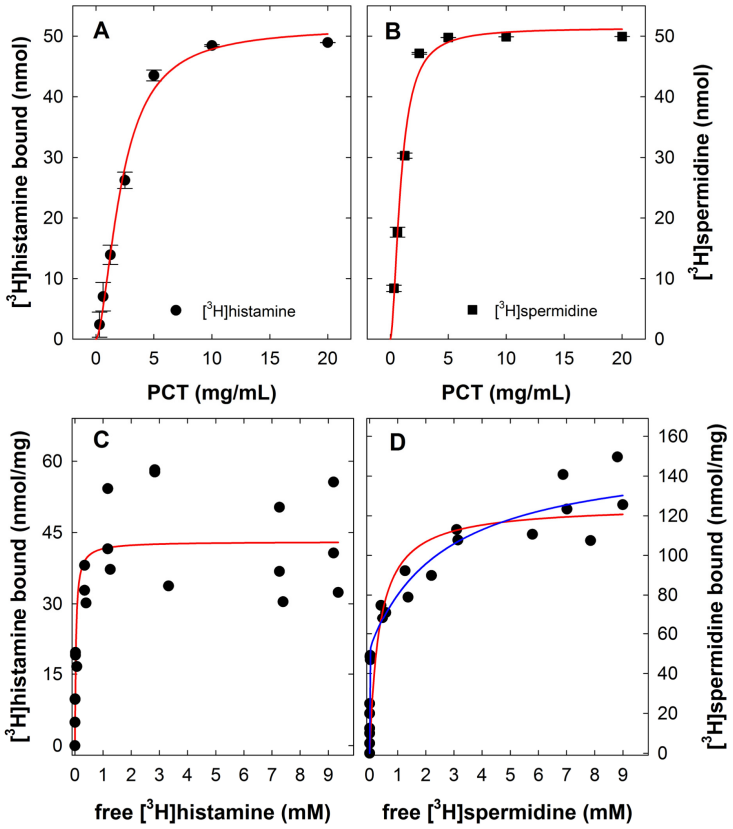

Figure 2. Titration of purified clinoptilolite-tuff (PCT) at a constant concentration of [^{3}H]histamine (**A**) and of [^{3}H]spermidine (**B**) and saturation binding of [^{3}H]histamine (**C**) and [^{3}H]spermidine (**C**) to PCT. (**A**,**B**) The binding reaction was carried out in a final volume of 0.5 mL containing PBS, the indicated concentrations of PCT and 100 µM [^{3}H]histamine (**A**) or [^{3}H]spermidine (**B**) (specific activity adjusted by isotopic dilution with unlabeled histamine or spermidine to about 2000 cpm/nmol). The incubation was for 2 h at 25 °C. Samples were subsequently processed as outlined in the legend in Figure 1 and Materials and Methods. Data are means ± S.D. from three independent experiments, which were performed in duplicate. The solid lines were drawn by fitting the Hill equation (three-parameter logistic equation) to the data points. (**C**,**D**) The binding reaction was carried out in a final volume of 0.5 mL containing PBS, 4 mg PCT and concentrations of [3H]histamine (panel **A**) or [3H]spermidine (panel **B**) ranging from 3 nM to 10 mM. The specific activity of the radioligands was adjusted by isotopic dilution with unlabeled histamine or spermidine. The incubation was for 2 h at 25 °C. Data are from three independent experiments, which were performed in duplicate. The red lines were drawn by curve fitting using the equation describing binding to a single site. The blue line in panel **D** resulted from curve fitting assuming the presence of two binding sites. This fit was significantly better (F = 48.3, $p < 0.001$; F-test).

2.2. Displacement of [^{3}H]histamine and [^{3}H]spermidine

Histamine and the polyamines spermine and spermidine share a common structural feature, i.e., two amines separated by three carbons. In putrescine (the precursor of spermidine and spermine) and in cadaverine, the two primary amines are separated by four and five carbon atoms, respectively. Spermidine and spermine harbor one and two additional amine nitrogens, respectively. We compared the ability of all five compounds to displace [^{3}H]histamine (Figure 3A) and [^{3}H]spermidine (Figure 3B) from PCT under equilibrium conditions. For displacement of [^{3}H]histamine binding, we observed a rank order of potency spermine = spermidine > cadaverine > histamine = putrescine (Table 1). In contrast, the compounds displaced [^{3}H]spermidine binding to PCT with a rank order of potency spermine > spermidine > putrescine = cadaverine (Table 1). Surprisingly, histamine failed to displace [^{3}H]spermidine from PCT even when present at 10 mM (circles in Figure 3B). This indicates that the binding sites for histamine and spermidine are not equivalent.

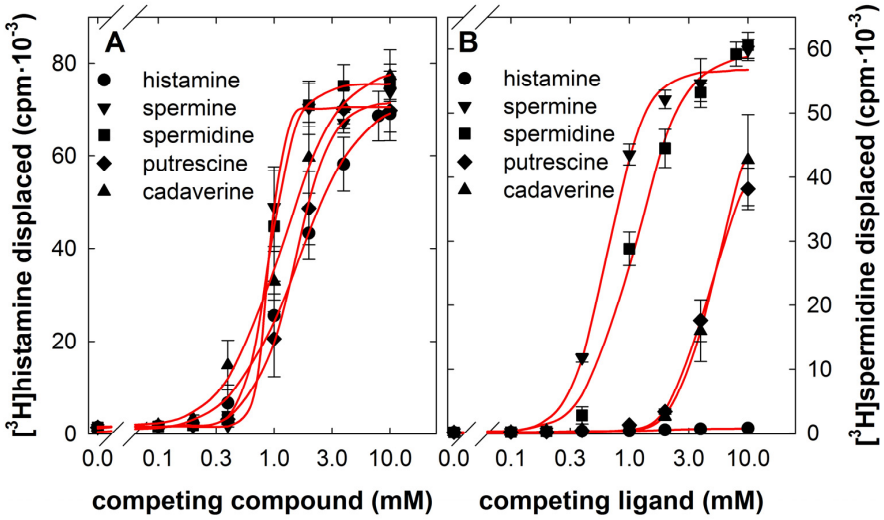

Figure 3. Competition by cadaverine, histamine, putrescine, spermidine and spermine for binding of [^{3}H]histamine (**A**) and [^{3}H]spermidine (**B**) to purified clinoptilolite-tuff (PCT). The binding reaction was carried out in a final volume of 0.5 mL containing PBS, 4 mg PCT, 8.8 nM [^{3}H]histamine (panel **A**) or 3 nM [^{3}H]spermidine (panel **B**) and the indicated concentrations of cadaverine (upward triangles), histamine (circles), putrescine (diamonds), spermidine (squares) or spermine (downward triangles). The incubation was for 2 h at 25 °C. Samples were subsequently processed as outlined in the legend in Figure 1 and Materials and Methods. Data are means ± S.D. from three independent experiments carried out in duplicate. The lines were drawn by fitting the Hill equation to the data points.

Table 1. Apparent affinities of cadaverine, histamine, putrescine, spermidine and spermine for displacing binding of [^{3}H]histamine, [^{3}H]spermidine and [^{3}H]cadaverine to PCT *.

	Displacement of					
	[^{3}H]histamine Binding		**[^{3}H]spermidine Binding**		**[^{3}H]cadaverine Binding**	
	IC_{50} (μM)	**Slope Factor**	**IC_{50} (μM)**	**Slope Factor**	**IC_{50} (μM)**	**Slope Factor**
cadaverine	1024 ± 24	1.6 ± 0.1	5357 ± 1000	2.9 ± 0.3	470 ± 123	1.6 ± 0.2
histamine	1389 ± 198	1.6 ± 0.2	n.c.	n.c.	n.c.	n.c.
putrescine	1423 ± 310	3.0 ± 1.0	4569 ± 541	2.9 ± 0.3	2153 ± 455	2.1 ± 0.3
spermidine	819 ± 59	3.5 ± 0.5	1127 ± 78	2.1 ± 0.1	663 ± 212	2.2 ± 0.2
spermine	785 ± 41	5.0 ± 0.7	662 ± 4	2.7 ± 0.1	473 ± 194	3.7 ± 0.2

* IC_{50} values and slope factors (Hill coefficients) were extracted from the fitted curves of the experiments summarized in Figures 3 and 4 Data are means ± S.D. (n = 3); n.c., not calculated, because histamine (up to 10 mM) failed to displace [^{3}H]spermidine and only displaced <<50% [^{3}H]cadaverine. Note that the IC_{50} values refer to the total concentration of the displacing ligands and do not take into account their depletion resulting from their binding to PCT. Thus, they reflect relative rather than absolute affinities.

The displacement curves differed in steepness, which is also evident from the slope factors (=Hill coefficients) summarized in Table 1. It is worth pointing out that the IC_{50} calculations are based on the total concentration of added competitors rather than their free concentration. If a large fraction of the competitor is bound to clinoptilolite, its free concentration is greatly reduced. The depletion of competing ligands (and thus the discrepancy between free and total concentration) accounts—at least in part—for the apparent steepness of the displacement curves. In addition, because of the depletion of competing ligands, the IC_{50} values greatly underestimate their true affinity. This is most readily evident if the IC_{50} values of histamine estimated from self-competition (1398 μM) are compared to the K_D value (36 μM) calculated from the saturation experiment shown in Figure 2C. Thus, the IC_{50} values only allow for gauging the relative affinity of the competing compounds.

2.3. Binding and Displacement of [^{3}H]cadaverine

The sorption of the diamines cadaverine and putrescine by PCT is of particular interest for the treatment of fungating wounds. As outlined above, the displacement experiments summarized in Figure 3 do not provide any information on the affinity of PCT for cadaverine or putrescine. In addition, the binding capacity cannot be inferred from the displacement of [^{3}H]histamine or [^{3}H]spermidine. In wound exudates obtained from fungating wounds, the cadaverine concentration exceeds that of putrescine by about 5-fold [16]. Hence, we examined the binding of radiolabeled cadaverine to PCT. The binding of both carrier-free [^{3}H]cadaverine (Figure 4A) and 100 μM [^{3}H]cadaverine (Figure 4B) was also rapid and remained stable for at least two hours. Saturation experiments revealed that binding of [^{3}H]cadaverine to PCT was better described by assuming the presence of two binding sites (blue curve in Figure 4C) than of a single binding site (red curve in Figure 4C): the following parameter estimates were extracted from the fit to the two-site model: $K_{D,1} = 7.2 \pm 6.8$ μM, $B_{max,1} = 26.5 \pm 5.4$ nmol/mg and $K_{D,2} = 14.1 \pm 11.4$ mM, $B_{max,2} = 247.2 \pm 120.6$ nmol/mg, for the high-and low-affinity components, respectively.

The structure–activity relation for displacing [^{3}H]cadaverine from PCT differed from that observed for displacing [^{3}H]histamine and [^{3}H]spermidine (cf. Figure 3A,B and Figure 4D): the rank order of potency was cadaverine = spermine > spermidine > putrescine > histamine (Table 1 and Figure 4D).

2.4. Binding of [^{3}H]cadaverine in the Presence of Wound Drainage Fluid

Wound exudates from fungating wounds contain cadaverine concentrations, which range from 0.1 to 1 mM [16,17]. In addition, wound exudates contain many additional compounds, which may be adsorbed to PCT and thus interfere with its capacity to bind cadaverine; this includes spermine in the micromolar range [29]. We obtained drainage fluid collected from surgical wounds of patients, who had undergone operations for breast cancer, and determined the amount of PCT required to bind 100 μM [^{3}H]cadaveri-ne in the absence (i.e., in PBS) and presence of wound drainage fluid. We selected this concentration of [^{3}H]cadaverine because it corresponded to the lower range of cadaverine concentrations found in exudates of fungating wounds [16,17] and would thus allow for detecting competition by compounds present in the exudates. It is evident from Figure 5A,C that the amount of PCT required to bind 50% of [^{3}H]cadaverine was not affected to any appreciable extent by any one of the seven wound drainage fluids tested.

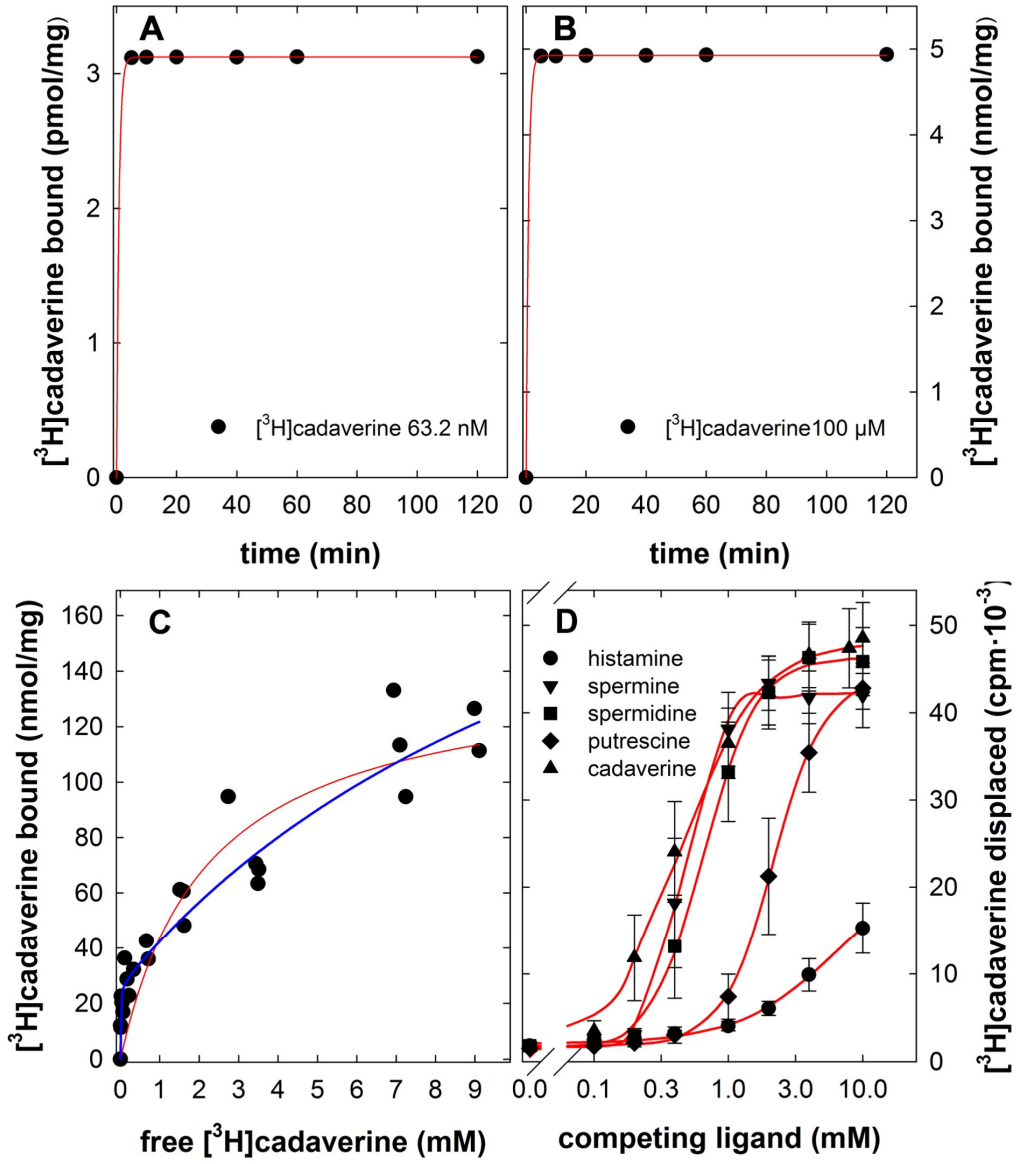

Figure 4. Time course (**A**,**B**) and saturation binding of [^{3}H]cadaverine (**C**) and competition by cadaverine, histamine, putrescine, spermidine and spermine (**D**) for binding of [^{3}H]cadaverine to purified clinoptilolite-tuff (PCT). (**A**,**B**) The binding reaction was carried out in a final volume of 0.5 mL containing PBS, 10 mg PCT and either carrier-free [^{3}H]cadaverine (i.e., 68 nM, specific activity 2.2 Ci/mmol, panel **A**) or [^{3}H]cadaverine isotopically diluted with unlabeled cadaverine (panel **B**) to yield a concentration of 100 µM. Samples were subsequently processed as outlined in the legend in Figure 1 and Materials and Methods. Data are from a representative experiment carried out in duplicate. (**C**) The binding reaction was carried out in a final volume of 0.5 mL containing PBS, 4 mg PCT and concentrations of [^{3}H]cadaverine ranging from 50 nM to 10 mM. The specific activity of the radioligand was adjusted by isotopic dilution with unlabeled cadaverine. The incubation was for 2 h at 25 °C. Data are from three independent experiments, which were performed in duplicate. The red and blue lines were drawn by curve fitting using the equations describing binding to a single site and two sites, respectively. The fit was significantly improved by positing two binding sites ($F = 17.6$, $p < 0.001$; F-test). (**D**) The binding reaction was carried out as in panel **C** with 42 nM [^{3}H]cadaverine and the indicated concentrations of cadaverine (upward triangles), histamine (circles), putrescine (diamonds), spermidine (squares) or spermine (downward triangles). Data are means ± S.D. from three independent experiments carried out in duplicate. The lines were drawn by fitting the Hill equation to the data points.

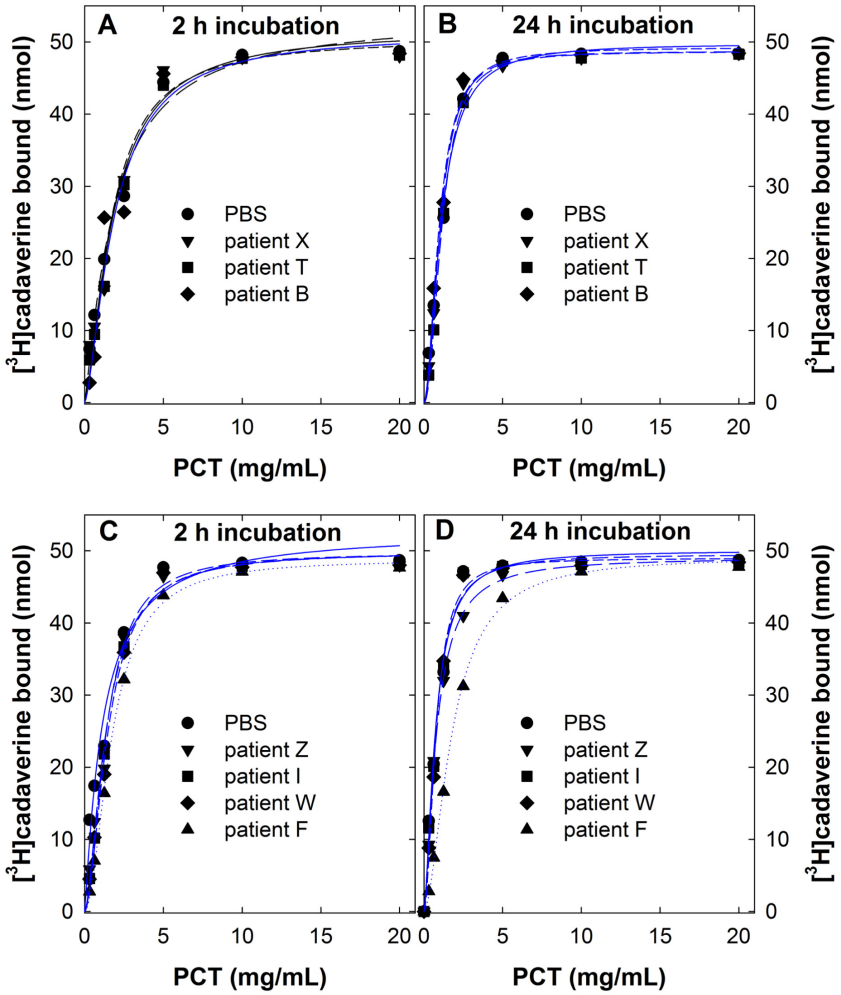

Figure 5. Titration of purified clinoptilolite-tuff (PCT) at a constant concentration of [^{3}H]cadaverine (100 μM) in the absence and presence of wound drainage fluid. The binding reaction was carried out in a final volume of 0.5 mL containing PBS, the indicated concentrations of PCT, 100 μM [^{3}H]cadaverine (specific activity adjusted by isotopic dilution with unlabeled cadaverine to about 2000 cpm/nmol) and 0.25 mL of exudate recovered by wound drainage from individual patients undergoing surgery for breast cancer. The incubation was carried out for 2 h (panels **A** and **C**) and for 24 h (panels **B** and **D**) at 25 °C. Samples were subsequently processed as outlined in the legend in Figure 1 and Materials and Methods. Data are from two independent experiments, which were performed in duplicate. The lines were drawn by fitting the Hill equation (three-parameter logistic equation) to the data points.

Wound dressings are not exchanged after 2 h, i.e., the incubation time employed in the experiments summarized in Figure 5A,C, but they are typically left for one day to cover a wound. Accordingly, we also examined the binding capacity after an incubation time of 24 h. As can be seen from Figure 5B,D, all curves but one (i.e., that for the fluid from patient F, upward triangles in Figure 5C,D) were shifted to the left. This is further illustrated in Figure 6A, which compares the apparent K_D values (=concentration of PCT suspension required to bind 50% of 100 μM [^{3}H]cadaverine) after an incubation time of 2 h and 24 h: the apparent K_D was lower in all but one instance (highlighted by the red symbol in Figure 6A), resulting in a median of 1.69 mg/mL (95% confidence interval 1.15–1.86) and 0.98 mg/mL (95% confidence interval 0.73–2.07) after a 2 h and 24 h incubation, respectively. In contrast, the binding capacity was comparable (Figure 6B), because essentially all [^{3}H]cadaverine was bound at saturating concentrations of PCT. We stress that these wound drainage fluids differed substantially in composition, which was already evident from their visual inspection and which is illustrated by the photograph of four representative samples in Figure 6.

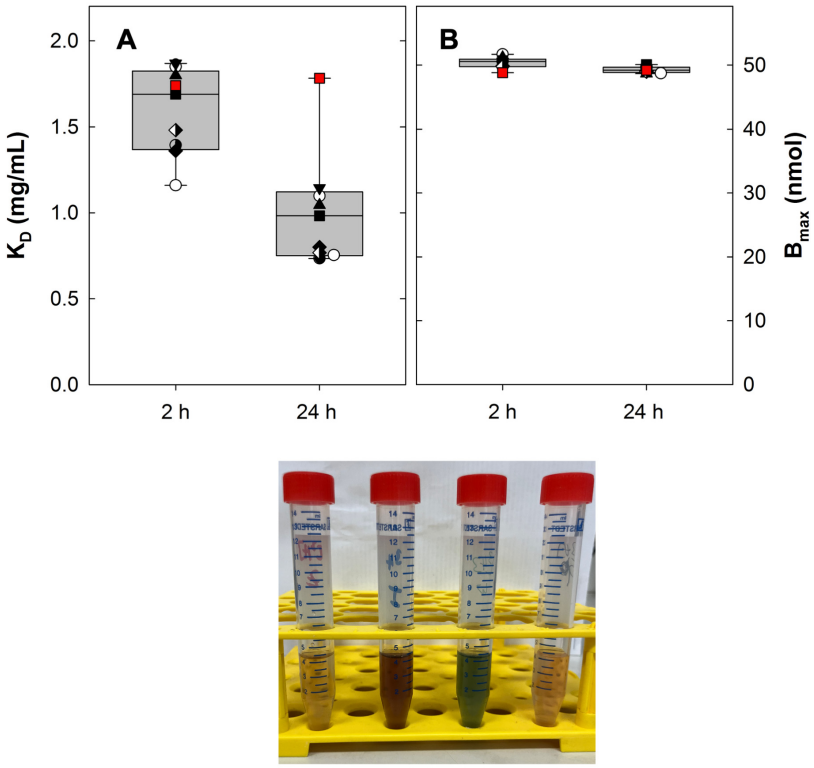

Figure 6. Effect of the incubation time on the apparent affinity (**A**) and the binding capacity (**B**) of purified clinoptilolite-tuff (PCT) for [^{3}H]cadaverine. The K_D values (concentration of PCT required to bind 50% of 100 µM [^{3}H]cadaverine, panel **A**) and the binding capacity B_{max} (panel **B**) were extracted from the individual curves shown in Figure 7. The box plot illustrates the median and the interquartile range, whiskers indicate the 95% confidence interval. The control values measured in PBS are indicated by open circles. The red symbol indicates the outlier (wound drainage fluid of patient F), where the 24 h incubation did not enhance the apparent affinity. In spite of this outlier, a paired comparison of the K_D values determined after the 2 h and the 24 h incubation indicated that the apparent affinity was significantly higher after the 24 h incubation (p = 0.008, Wilcoxon signed-rank test). The photograph shows 4 representative wound drainage fluids to illustrate the variability in color and thus in chemical composition.

2.5. Binding of [^{3}H]cadaverine to PCT-Containing Wound Dressing

In a phase I trial, the current preparation of PCT has been shown to be safe, when directly applied to artificial wounds [18]. However, PCT is likely to be more effective and easily applicable if incorporated into wound dressing, because this precludes deposition onto the granulation tissue and incorporation into the dermis [18]. Accordingly, a prototype was generated (by SFM, Speciality Fibres and Materials Ltd., Coventry, UK), where PCT was incorporated into an alginate/cellulose compound wound dressing. Squares of 1 × 1 cm dimension weighed 15 mg and thus contained about 0.7 mg PCT. We, therefore, compared the binding of [^{3}H]cadaverine to 1 × 1 cm pieces of PCT-doped wound dressing with that of 0.7 mg free PCT in suspension. The concentration range of [^{3}H]cadaverine covered the relevant range of 0.1 to 1 mM [16,17]. The experimental observations showed that—within experimental error—the PCT-doped alginate wound dressing (triangles in Figure 7) and the PCT suspension (circles in Figure 7) adsorbed equivalent amounts of [^{3}H]cadaverine. Accordingly, the red and black curves in Figure 7 were virtually superimposable. In contrast, neither the control alginate wound dressing (diamonds in Figure 7) nor the cellulose-based control wound dressing (squares in Figure 7) bound appreciable amounts of [^{3}H]cadaverine over the concentration range studied.

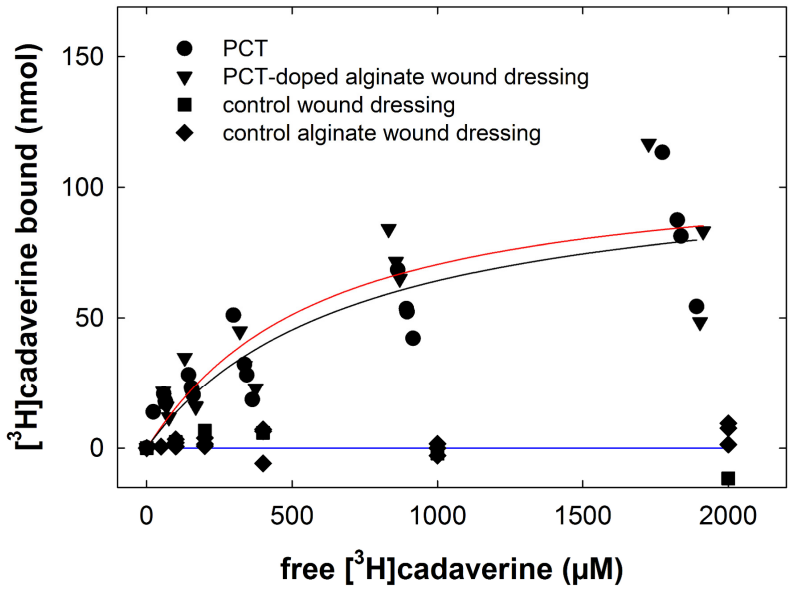

Figure 7. [^{3}H]Cadaverine binding to purified clinoptilolite-tuff (PCT) in solution and to PCT-doped wound dressing. The binding reaction was carried out in a final volume of 0.5 mL containing PBS, 0.7 mg PCT (circles), 1 × 1 cm squares of PCT-doped alginate wound dressing (triangles) of control alginate wound dressing (diamonds) or a cellulose-based control wound dressing (squares) and concentrations of [^{3}H]cadaverine ranging from 50 nM to 2 mM. The specific activity of the radioligand was adjusted by isotopic dilution with unlabeled cadaverine. The incubation was for 2 h at 25 °C. Samples were subsequently processed as outlined in the legend in Figure 1 and Materials and Methods. Data are from three to four independent experiments, which were performed in duplicate. The black (PCT-doped wound dressing) and red line (PCT in suspension) were drawn by curve fitting using the Hill equation.

3. Discussion

The natural zeolite clinoptilolite is a versatile sorbent that is exploited in industrial and agricultural applications and for food production [30,31]. The preparation of purified clinoptilolite-tuff used in this work has been extensively characterized both from a geoscientific perspective [32,33] and with respect to potential therapeutic applications: It is depleted of trace heavy metal contaminants [19] and accordingly, when ingested, suitable to prevent intestinal absorption of toxic metals. This was verified in a phase I trial with lead [34]. Adsorption is not limited to small cations, but the micronized purified clinoptilolite-tuff preparation also effectively removes bacterial toxins [35], allergens [21,22], bile acids [35] and viruses [23,24] and is efficacious in mitigating experimental colitis [36]. Finally, its safety in wound management was also demonstrated in a phase I trial with artificial wounds [24]. The time course of acute wound healing is predictable and requires limited medical care [37], but chronic wounds—in particular, malignant fungating wounds—represent a challenge. We conclude that this preparation of purified clinoptilolite-tuff has several useful properties, which make it an attractive alternative to the currently available treatment options for malodor associated with fungating wounds. This conclusion is based on the following observations: (i) purified clinoptilolite-tuff bound diamines and polyamines rapidly with high capacity, (ii) the binding affinities of the three examined ligands—[^{3}H]cadaverine, [^{3}H]histamine and [^{3}H]spermidine—were in the low μM range and (iii) the binding sites were non-equivalent. These three properties combined to support effective binding for any given ligand in the presence of the expected, submillimolar concentrations of competing ligands. In fact, binding of [^{3}H]cadaverine was maintained in the presence of copious amounts of wound drainage fluids, which contain a heterogenous mixture of potential competitors. (iv) In addition, the binding of [^{3}H]cadaverine was stable

for at least 24 h in the presence of wound drainage fluids. (v) Finally, [^{3}H]cadaverine was effectively adsorbed by a wound dressing, into which purified clinoptilolite-tuff had been incorporated: the observed binding capacity of this wound dressing was consistent with its content of purified clinoptilolite-tuff.

The crystal lattice of clinoptilolite has a net negative charge allowing for cation exchange and adsorption on the surface of the crystal and within the crystal structure [30]. Accordingly, it is not surprising that diamines and polyamines were readily bound by the preparation of purified clinoptilolite-tuff. However, adsorption to purified clinoptilolite-tuff was not solely driven by electrostatic interactions. Three arguments support the conjecture that the binding sites are heterogenous and non-equivalent: (i) Binding of [^{3}H]histamine occurred to a single class of homogeneous binding sites; in contrast, the saturation curves for both [^{3}H]spermidine and [^{3}H]cadaverine were incompatible with binding to a single site. The difference in binding site density is illustrated in Figure 8A: it is evident that the [^{3}H]histamine binding capacity (43 nmol/mg) was lower than the binding capacity for [^{3}H]spermidine (sum of $B_{max,1}$ and $B_{max,2}$ = 153 nmol/mg) and [^{3}H]cadaverine (sum of $B_{max,1}$ and $B_{max,2}$ = 273 nmol/mg). (ii) [^{3}H]Histamine was displaced by all compounds tested. In contrast, unlabeled histamine was ineffective in displacing [^{3}H]spermidine and only poorly displaced [^{3}H]cadaverine. (iii) Similarly, the structure–activity relation of diamines and polyamines differed substantially in their ability to displace [^{3}H]spermidine and [^{3}H]cadaverine: the difference in inhibitory potency can be illustrated by calculating the pairwise ratio of IC_{50} for all compounds other than histamine (for which IC_{50} values in displacing [^{3}H]spermidine and [^{3}H]cadaverine could not be determined). As shown in Figure 8B, unlabeled cadaverine was 11.3- and 5.2-fold more potent in self-competition than in displacing [^{3}H]spermidine (red bar indicating S/C ratio in Figure 8B). Unlabeled cadaverine was also 5.2-fold more potent in competing with [^{3}H]histamine than with [^{3}H]spermidine (green bar indicating S/H ratio in Figure 8B) and two-fold more potent in self-competition than in displacing [^{3}H]histamine (blue bar indicating S/H ratio in Figure 8B). Similarly, large differences in potency ratios were observed with putrescine, which was, e.g., 3.2-fold in competing for the binding of [^{3}H]histamine than for that of [^{3}H]spermidine (green bar indicating S/H ratio in Figure 8B). In contrast, for both spermidine and spermine, the IC50 ratios were less pronounced, i.e., ranging from 1.7 to 0.6-fold (cf. also Table 1) and thus not substantially different from unity (indicated by the black line in Figure 8B).

It is worth pointing out that depletion of the unlabeled ligand cannot account for the 10-fold higher potency in displacing [^{3}H]cadaverine than [^{3}H]spermidine because the same amount of purified clinoptilolite-tuff was used in these experiments. Thus, the extent of depletion—i.e., the reduction in free concentration—must have been similar. Finally, irrespective of the radioligand used to label the binding sites, spermine was consistently the most potent displacing agent (cf. Table 1). Taken together, these findings provide circumstantial evidence for the following speculative model: [^{3}H]spermidine occupies binding sites, which can accommodate two, three or more linearly arranged nitrogen atoms with differing affinities. In contrast, [^{3}H]cadaverine preferentially labels binding sites, which accommodate two linearly spaced nitrogen atoms. This may account for the large difference in potency between self-competition (of cadaverine) and displacement of [^{3}H]spermidine (by cadaverine). The distance between the nitrogen atoms is relevant because putrescine (1,4-diaminobutane) was less potent than cadaverine (1,5-diaminopentane). Spermine with its four linearly arranged nitrogen amines binds with high affinity to all binding sites. The imidazole ring of histamine may restrict its access to some binding sites. This provides an explanation for its inability to compete for the binding of [^{3}H]spermidine and [^{3}H]cadaverine and for the lower binding capacity of PCT for histamine. We stress that our

conjecture about binding heterogeneity remains a hypothesis based on indirect evidence: further studies employing advanced techniques such as X-Ray powder diffraction are required to verify the binding properties and the heterogeneity of binding sites in PCT at the molecular or structural level.

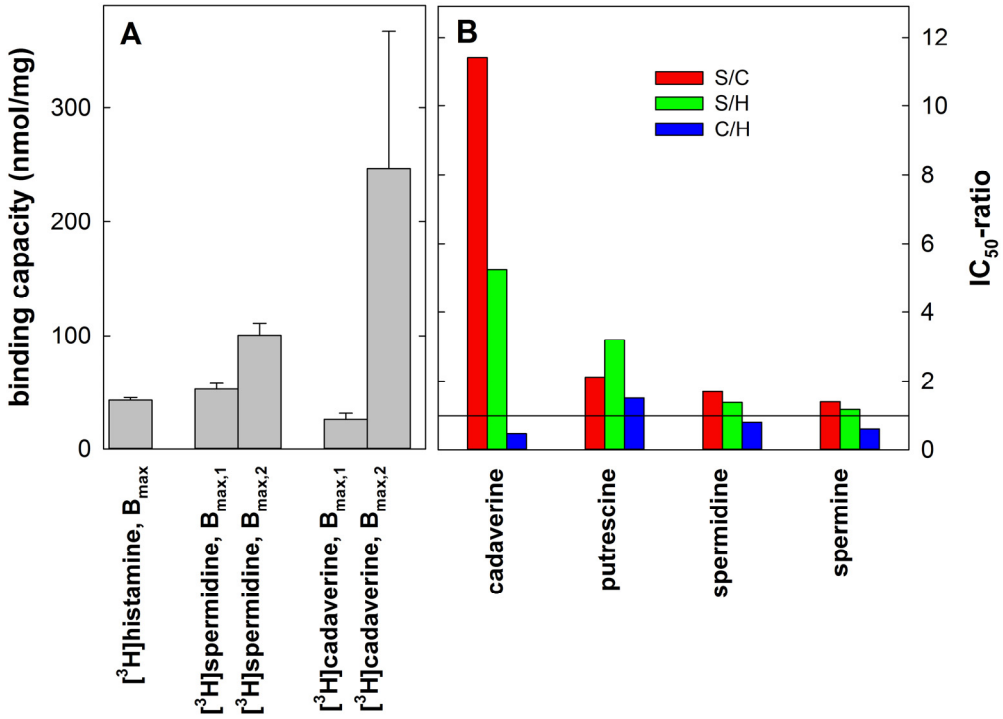

Figure 8. Comparison of the binding capacity of purified clinoptilolite-tuff (PCT) for [^{3}H]histamine, [^{3}H]spermidine and [^{3}H]cadaverine (**A**) and the potency ratios of cadaverine, putrescine, spermidine and spermine (**B**). (**A**) The binding capacity corresponds to the B_{max} values extracted from the fitted curves shown in Figures 2C,D and 4C. (**B**) The ratios of IC_{50} were calculated from the data compiled in Table 1, where S/C, S/H and C/H represent the potency ratios of the cadaverine, putrescine, spermidine and spermine for competing for binding of [^{3}H]spermidine vs. [^{3}H]cadaverine, [^{3}H]spermidine vs. [^{3}H]histamine and [^{3}H]cadaverine vs. [^{3}H]histamine, respectively. The black line indicates an IC_{50} ratio of 1, which is to be expected if a compound competes with equal potency for the indicated radiolabeled tracers.

The adsorption kinetics of cadaverine to charcoal-coated or aldehyde-functionalized cellulose and their combination were recently determined [17]: the binding equilibrium was reached after ≥4 h. Consistent with these slow binding kinetics, the affinity, which can be estimated from the available data, is in the range of 32 mM, >100 mM and 65 mM for charcoal-coated cellulose, for aldehyde functionalized cellulose and their combination, respectively [17]. Thus, the indirect comparison of the data from Wen et al. [17] and of our observations indicates that clinoptilolite depletes cadaverine from the solution substantially more rapidly and with higher affinity than charcoal-coated cellulose, aldehyde-functionalized cellulose or a combination thereof.

Cutaneous wound healing is initiated by blood clotting and proceeds in three interlocking phases, i.e., inflammation, proliferation and remodeling [37,38]: the initial inflammatory response is dependent on the recruitment of leucocytes (macrophages, neutrophils, mast cells) and the exudation of blood constituents. Histamine supports fluid exudation. Accordingly, wound healing is delayed in mice deficient in histidine decarboxylase [39]. However, histamine also impairs skin barrier function by engaging both H_1- and H_2- receptors [40]. Arguably, the adsorption of histamine by PCT may impair the initial phase of wound healing. In chronic wounds, though, moisture-associated dermatitis and the resulting

impaired skin barrier are more important. In addition, histamine is a virulence factor for several bacterial species including *Pseudomonas aeruginosa* [27]. Thus, in chronic wounds, the removal of histamine by PCT is likely beneficial. Similarly, polyamine synthesis is required for keratinocyte migration during wound healing [41] and topical spermidine promotes wound healing [42]. However, spermidine is a double-edged sword: the growth of many bacteria including *Pseudomonas aeruginosa* is promoted by spermidine. In addition, and importantly, spermidine can confer bacterial resistance to antibiotics [43,44]. Hence, it is justified to posit that, in chronic fungating wounds, the benefits associated with the removal of cadaverine, putrescine, spermidine and spermine by PCT outweigh any potential negative effect arising from the depletion of spermidine in the exudate. This conjecture is supported by a phase I trial: the re-epithelization of artificial wounds was not impeded by the direct application of micronized purified PCT to the wound surface [26].

Our study has several limitations: (i) Wound fluids are heterogenous. We did not have access to exudate from fungating wounds, but used wound exudates collected from patients who had undergone breast cancer surgery. We cannot formally rule out that constituents of fungating wound exudates interfere with the binding of cadaverine and putrescine. However, it is worth pointing out that the binding capacity of PCT is large. In fact, the goal is to provide a wound dressing where the amount of available binding sites exceeds the mass of potential ligands. Under these conditions, possible competition for common binding sites becomes irrelevant. In fact, our assay conditions mimic this situation. This is evident from the large discrepancy, which we observed in the binding affinity determined in saturation experiments and the IC_{50} estimated from the competition experiments. Under realistic conditions where 10 mL of fungating wound exudate contains 1 nmol to 10 nmol of cadaverine (that is 100 μM to 1 mM) [16], 1 mg of PCT is predicted to readily suffice for sorbing the cadaverine molecules and a large fraction of binding sites remain unoccupied and thus available to bind additional compounds. In the current prototype, 1.3 cm^2 of PCT-doped wound dressing provides 1 mg of PCT and thus suffices to adsorb a substantially larger amount than 10 nmol of cadaverine (or putrescine), but a wound of this size is unlikely to be covered with 10 mL of fluid. (ii) We also did not test the effect of varying pH and ionic strength on the adsorptive capacity. We consider ionic strength of modest interest because wound exudates have the same ionic composition as plasma [45]. There is a large variation in the pH of wound exudates [46]. Bacterially contamination results in wound exudate, which is alkaline [47,48]. The wound exudates that were collected and used were alkaline (average pH = 8.0). This did not affect the ability of PCT to bind cadaverines (cf. Figures 5 and 6). This was to be expected because the pKa of the amine groups of cadaverines is 9.1 and 10.2. Thus, variation in pH only has a modest effect on the ionization of cadaverine. (iii) We cannot rule out that the removal of solutes, which are present in wound fluids, may have a negative impact on wound healing. However, in cell culture, PCT did not affect the viability and the ohmic resistance of an epithelial cell layer [35]. Importantly, in a phase I trial with artificial wounds, the current preparation of micronized purified PCT did not affect wound closure [26].

Malodorous discharges are not limited to cancerous fungating wounds, they are also found in other chronic wounds—e.g., venous, arterial and diabetic foot ulcers[15]—and in hidradenitis suppurativa [49]. We show here that micronized purified clinoptilolite-tuff can be readily incorporated into a wound dressing without affecting its capacity to bind cadaverine. Thus, wound dressings containing PCT may allow for exploiting its adsorptive capacity while limiting the direct impact of clinoptilolite on cellular constituents of the granulation tissue [26]. In addition, clinoptilolite can be impregnated with silver ions to support a controlled release of Ag^+ [50]. Because the repugnant smell arises from bacterial colonization, this is predicted to further enhance the beneficial action of clinoptilolite-

containing wound dressings. We consider this approach worthwhile exploring given the limited currently available treatment options.

The scalability of incorporating PCT into wound dressings is promising. It can be integrated into wound care materials using standard production methods, such as mixing, impregnation or coating of fibers or the finished dressing. This allows the production of large quantities of functional wound dressings at a large scale and with consistent quality.

PCT is manufactured from a natural clinoptilolite-bearing high-grade raw material, which can be sourced sustainably and cost-effectively. PCT, derived through a quality-controlled refinement process, has undergone clinical evaluation in a phase I trial [26] and imparts enhanced properties to wound dressings. These properties expand their functionality, making them applicable in a broader range of advanced wound care solutions, including the adsorption of toxins, pathogens, inflammatory factors and excess fluids. Future research will investigate the potential of PCT-doped alginate dressings to bind and inactivate bacterial and viral pathogens. In addition, the focus will be on clinical evaluation in both chronic and acute wound settings.

4. Materials and Methods

4.1. Materials

Cadaverine dihydrochloride (1,5-diaminopentane; catalogue number C8561), histamine dihydrochloride (53300), putrescine (1,4-diaminobutane, D13208), spermine (85590) and spermidine (S2626) and buffer salts were purchased from Sigma-Aldrich (St. Louis, MO, USA). [^{3}H]Histamine (specific activity 16.4 Ci/mmol) and [^{3}H]spermidine (specific activity 36.4 Ci/mmol) were obtained from Perkin Elmer (Boston, MA, USA); [^{3}H]cadaverine (specific activity 2.2 Ci/mmol) was from Moravek (Brea, CA, USA).

The raw material of PCT originated from a mine in the eastern Slovak Republic [24,25]. The patented, validated and fully quality-controlled manufacturing process, which yielded micronized purified clinoptilolite-tuff (PCT), was previously described [33]. PCT was further immobilized in alginate fibers and blended with cellulose fibers in a non-woven wound dressing (Speciality Fibres and Materials Ltd., Coventry, UK). Control wound dressings included alginate fibers without PCT and cellulose fibers: PCT in particulate form was mixed into the alginate solution before extrusion, leading to a homogeneous distribution of PCT within the resulting calcium alginate fibers. In the subsequent production steps, the PCT-doped alginate fiber was combined with cellulose-type fibers, enhancing the mechanical strength as well as the absorbency characteristics of the final dressing. The integration of PCT does not adversely affect the ease of use, flexibility, weight, strength or integrity of the dressing.

4.2. Wound Drainage Fluid

Closed suction drainage specimens were collected at the Department of Surgery (Medical University of Vienna) from patients who had undergone breast cancer surgery. The University Ethics Committee approved the use of drainage fluid for experimental purposes (Ethics Committee submission number 2132/2013). The patients gave their informed consent in writing. Drainage flasks were retrieved the day after surgery, swiftly transferred to the laboratory and the contents cleared from particulate matter by centrifugation (5000× *g* for 10 min). The flasks held volumes between 10 and 100 mL, which typically included hematoma. The tinting of the cleared drainage fluid was between amber and black reflecting the degree of hemolysis that had occurred in the flask. Each specimen was labeled with a letter code rendering its source anonymous. Samples were stored frozen.

4.3. Binding Experiments

PCT was suspended in phosphate-buffered saline (137 mM NaCl, 2.7 mM KCl, 10 mM Na_2HPO_4, 2 mM KH_2PO_4, pH 7.4) to yield concentrations ranging from 40 mg/mL to 0.6 mg/mL. Binding reactions were performed in Eppendorf tubes in a final volume of 0.5 mL containing PBS, PCT (0.15 to 10 mg), radioactive ligands (0.05 to 0.1 μCi of [^{3}H]histamine, [^{3}H]spermidine or [^{3}H]cadaverine), competing compounds and in some instances, wound drainage fluid obtained from patients. During the incubation at 25 °C, samples were placed on a horizontal shaker and continuously shaken (120 min^{-1}). The experimental approach is summarized in the following schematic diagram:

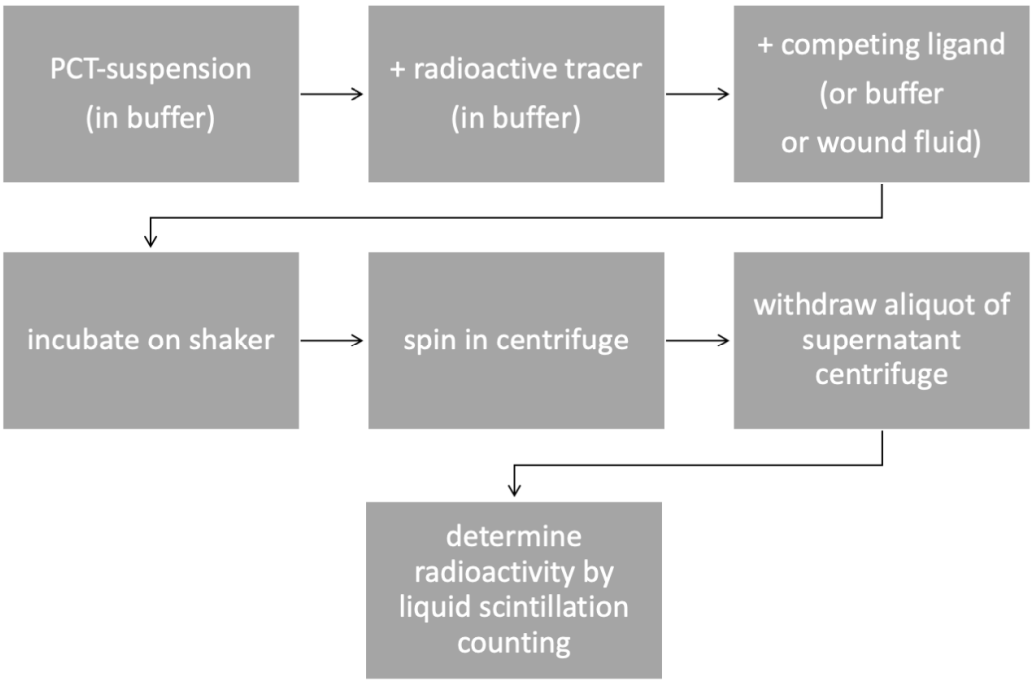

The following four different types of experiments were performed:

(i) In time course experiments, PCT (10 mg/assay) was mixed either with carrier-free radioactive ligands (resulting in concentrations in the nM range) or with radioactive ligands, which had been isotopically diluted with 100 μM of the unlabeled compound. The incubation time varied between 4 and 119 min. Bound and free radioligand were separated by centrifugation (1 min at 12,000× *g*). An aliquot of the supernatant (0.25 mL) was withdrawn and transferred to scintillation vials. The bound fraction was calculated by subtracting the free fraction determined in the supernatant from the total radioactivity added to the reaction.

(ii) In titration experiments, the amount of PCT varied between 0.15 and 10 mg. The concentration of each radioactive ligand (0.05 to 0.1 μCi) was adjusted to 100 μM by isotopic dilution with the unlabeled compound. When added, wound drainage fluid represented 50% of the reaction volume. The incubation was carried out for 2 h or 24 h. We separately determined the extent by which wound drainage fluid quenched liquid scintillation counting of radioactivity: regardless of their color, quenching was not seen if ≤50 μL of wound drainage fluid was added to the scintillation vial. Accordingly, in experiments that examined the effect of wound drainage fluid on the binding of [^{3}H]cadaverine to PCT, a 50 μL aliquot was withdrawn to measure the amount of free radioactivity remaining in the supernatant.

(iii) In saturation experiments, PCT (4 mg/reaction) was incubated for 2 h with increasing concentrations of each radioactive ligand. The total radioactivity (0.05 to 0.1 μCi) was

kept constant, and the specific activity was progressively diluted by the addition of an unlabeled ligand (0.1 to 10 mM). Saturation experiments were also performed to compare the binding of [^{3}H]cadaverine (0.08 μCi carrier-free and diluted with 0.05 to 2 mM unlabeled cadaverine) to 0.7 mg PCT in suspension with the binding to squares (1 × 1 cm) of PCT-doped wound dressing, alginate wound dressing (PCT free) or control wound dressing.

(iv) Finally, in competition experiments, PCT (4 mg/reaction) was incubated in the presence of each radioactive ligand (0.05 to 0.1 μCi) and increasing concentrations of unlabeled cadaverine, histamine, putrescine, spermidine or spermine for 2 h. Preliminary experiments (with total concentrations increasing by one order magnitude from 1 nM to 10 mM) were carried out to identify the concentration range, where the compounds competed effectively with the radiolabeled tracers. Because total concentrations $\leq$ 0.1 mM failed to displace the bound radiotracers, logarithmically concentrations covering the range of 0.1 to 10 mM were subsequently to determine the inhibitory potency of competitors.

In titration, saturation and competition experiments, the reaction was also terminated by centrifugation (5 min at 12,000× *g*) to separate bound and free radioactivity. The free radioactivity was determined in the supernatant by scintillation counting and the bound radioactivity was estimated as outlined above by subtracting the free radioactivity in the supernatant from the total radioactivity.

4.4. Statistics

The Hill equation (three-parameter logistic equation) and the appropriate equations for a rectangular hyperbola for the sum of two hyperbolae and a mono-exponential rise were used for non-linear, least-squares curve fitting to calculate the parameter estimates. An F-test based on the extra-sum-of-square principle verified if the fit was improved by assuming the presence of two rather than one binding site. Statistical comparisons between incubations performed for 2 and 24 h were carried out by a paired *t*-test or by a Wilcoxon signed-rank test.

Author Contributions: Conceptualization, M.F., C.N., C.T. and S.N.; methodology, A.E.-K., M.F. and C.N.; validation, M.F., C.N. and C.T.; formal analysis, M.F.; investigation, A.E.-K. and M.F.; resources, C.N., C.T. and S.N.; data curation, M.F. and C.N.; writing—original draft preparation, M.F.; writing—review and editing, S.N. and C.T.; visualization, M.F.; supervision, M.F.; project administration, M.F. and C.T.; funding acquisition, M.F. and C.T. All authors have read and agreed to the published version of the manuscript.

Funding: This research was funded by a grant from Value Privatstiftung.

Institutional Review Board Statement: This study was conducted in accordance with the Declaration of Helsinki, and approved by the Institutional Review Board (or Ethics Committee). The use of drainage fluid for experimental purposes was approved by the Ethics Committee of the Medical University of Vienna (Ethics Committee submission number 2132/2013).

Informed Consent Statement: Informed consent was obtained from all patients whose drainage fluid was collected.

Data Availability Statement: All data generated and analyzed are included in the published article. Primary data are available on request.

Conflicts of Interest: Ali El-Kasaby, Christian Nanoff and Michael Freissmuth declare no conflicts of interest. Cornelius Tschegg and Stephane Nizet are employees of GLOCK Health, Science and Research GmbH, which has a commercial interest in purified clinoptilolite-tuff. The funder had no role in the design of the study; in the collection, analysis, or interpretation of data; in the writing of the manuscript; or in the decision to publish the results.

References

1. Abrams, H.L.; Sprio, R.; Goldstein, N. Metastases in carcinoma; analysis of 1000 autopsied cases. *Cancer* **1950**, *3*, 74–85. [CrossRef]
2. McWhorter, J.E.; Cloud, A.W. Malignant tumors and their metastases: A summary of the necropsies on eight hundred sixty-five cases performed at the Bellevue hospital of New York. *Ann. Surg.* **1930**, *92*, 434–443. [CrossRef] [PubMed]
3. Gates, O. Cutaneous Metastases of Malignant Disease. *Am. J. Cancer* **1937**, *30*, 718–730.
4. Lookingbill, D.P.; Spangler, N.; Helm, K.F. Cutaneous metastases in patients with metastatic carcinoma: A retrospective study of 4020 patients. *J. Am. Acad. Dermatol.* **1993**, *29*, 228–236. [CrossRef] [PubMed]
5. Probst, S.; Arber, A.; Faithfull, S. Malignant fungating wounds: A survey of nurses' clinical practice in Switzerland. *Eur. J. Oncol. Nurs.* **2009**, *13*, 295–298. [CrossRef] [PubMed]
6. Tilley, C.P.; Fu, M.R.; Qiu, J.M.; Comfort, C.; Crocilla, B.L.; Li, Z.; Axelrod, D. The microbiome and metabolome of malignant fungating wounds: A systematic review of the literature from 1995 to 2020. J. *Wound Ostomy Cont. Nurs.* **2021**, *48*, 124–135. [CrossRef] [PubMed]
7. Vardhan, M.; Flaminio, Z.; Sapru, S.; Tilley, C.P.; Fu, M.R.; Comfort, C.; Li, X.; Saxena, D. The microbiome, malignant fungating wounds, and palliative care. *Front. Cell. Infect. Microbiol.* **2019**, *9*, 373. [CrossRef] [PubMed]
8. Fleck, C.A. Fighting odor in wounds. *Adv. Ski. Wound Care* **2006**, *19*, 242–244. [CrossRef]
9. Fromantin, I.; Seyer, D.; Watson, S.; Rollot, F.; Elard, J.; Escande, M.C.; De Rycke, Y.; Kriegel, I.; Larreta Garde, V. Bacterial floras and biofilms of malignant wounds associated with breast cancers. *J. Clin. Microbiol.* **2013**, *51*, 3368–3373. [CrossRef]
10. Michael, A.J. Polyamines in eukaryotes, bacteria, and archaea. *J. Biol. Chem.* **2016**, *291*, 14896–14903. [CrossRef] [PubMed]
11. Hussain, A.; Saraiva, L.R.; Ferrero, D.M.; Ahuja, G.; Krishna, V.S.; Liberles, S.D.; Korsching, S.I. High-affinity olfactory receptor for the death-associated odor cadaverine. *Proc. Natl. Acad. Sci. USA* **2013**, *110*, 19579–19584. [CrossRef]
12. Jia, L.; Li, S.; Dai, W.; Guo, L.; Xu, Z.; Scott, A.M.; Zhang, Z.; Ren, J.; Zhang, Q.; Dexheimer, T.S.; et al. Convergent olfactory trace amine-associated receptors detect biogenic polyamines with distinct motifs via a conserved binding site. *J. Biol. Chem.* **2021**, *297*, 101268. [CrossRef] [PubMed]
13. Wisman, A.; Shrira, I. The smell of death: Evidence that putrescine elicits threat management mechanisms. *Front. Psychol.* **2015**, *6*, 1274. [CrossRef] [PubMed]
14. Gethin, G.; Grocott, P.; Probst, S.; Clarke, E. Current practice in the management of wound odour: An international survey. *Int. J. Nurs. Stud.* **2014**, *51*, 865–874. [CrossRef]
15. Gethin, G.; Murphy, L.; Sezgin, D.; Carr, P.J.; Mcintosh, C.; Probst, S. Resigning oneself to a life of wound-related odour—A thematic analysis of patient experiences. *J. Tissue Viability* **2023**, *32*, 460–464. [CrossRef] [PubMed]
16. Tamai, N.; Akase, T.; Minematsu, T.; Higashi, K.; Toida, T.; Igarashi, K.; Sanada, H. Association between components of exudates and periwound moisture-associated dermatitis in breast cancer patients with malignant fungating wounds. *Biol. Res. Nurs.* **2016**, *18*, 199–206. [CrossRef]
17. Wen, J.; Almurani, M.; Liu, P.; Sun, Y. Aldehyde-functionalized cellulose as reactive sorbents for the capture and retention of polyamine odor molecules associated with chronic wounds. *Carbohydr. Polym.* **2023**, *316*, 121077. [CrossRef] [PubMed]
18. Akhmetova, A.; Saliev, T.; Allan, I.U.; Illsley, M.J.; Nurgozhin, T.; Mikhalovsky, S. A Comprehensive review of topical odor-controlling treatment options for chronic wounds. *J. Wound Ostomy Cont. Nurs.* **2016**, *43*, 598–609. [CrossRef]
19. Haemmerle, M.; Fendrych, J.; Matiasek, E.; Tschegg, C. Adsorption and release characteristics of purified and non-purified clinoptilolite-tuffs towards health-relevant heavy metals. *Crystals* **2021**, *11*, 1343. [CrossRef]
20. Haemmerle, M.M.; Tschegg, C. Sorption of Natural Siderophores onto clinoptilolite-tuff and its controlled-release characteristics. *Minerals* **2023**, *13*, 611. [CrossRef]
21. Ranftler, C.; Röhrich, A.; Sparer, A.; Tschegg, C.; Nagl, D. Purified clinoptilolite-tuff as an efficient sorbent for gluten derived from food. *Int. J. Mol. Sci.* **2022**, *23*, 5143. [CrossRef] [PubMed]
22. Ranftler, C.; Zehentner, M.; Pengl, A.; Röhrich, A.; Tschegg, C.; Nagl, D. Purified clinoptilolite-tuff as an efficient sorbent for food-derived peanut allergens. *Int. J. Mol. Sci.* **2024**, *25*, 6510. [CrossRef]
23. Nizet, S.; Rieger, J.; Sarabi, A.; Lajtai, G.; Zatloukal, K.; Tschegg, C. Binding and inactivation of human coronaviruses, including SARS-CoV-2, onto purified clinoptilolite-tuff. *Sci. Rep.* **2023**, *13*, 4673. [CrossRef]
24. Sarabi, A.; Nizet, S.; Röhrich, A.; Tschegg, C. Unveiling the broad-spectrum virucidal potential of purified clinoptilolite-tuff. *Microorganisms* **2024**, *12*, 1572. [CrossRef] [PubMed]
25. Schuster, I.; Bernhardt, R. Interactions of natural polyamines with mammalian proteins. *Biomol. Concepts* **2011**, *2*, 79–94. [CrossRef] [PubMed]
26. Deinsberger, J.; Marquart, E.; Nizet, S.; Meisslitzer, C.; Tschegg, C.; Uspenska, K.; Gouya, G.; Niederdöckl, J.; Freissmuth, M.; Wolzt, M.; et al. Topically administered purified clinoptilolite-tuff for the treatment of cutaneous wounds: A prospective, randomised phase I clinical trial. *Wound Repair Regen.* **2022**, *30*, 198–209. [CrossRef] [PubMed]
27. Krell, T.; Gavira, J.A.; Velando, F.; Fernández, M.; Roca, A.; Monteagudo-Cascales, E.; Matilla, M.A. Histamine: A bacterial signal molecule. *Int. J. Mol. Sci.* **2021**, *22*, 6312. [CrossRef]

28. Cooper, R.A.; Morwood, J.M.; Burton, N. Histamine production by bacteria isolated from wounds. *J. Infect.* **2004**, *49*, 39. [CrossRef]
29. Nanoff, C.; Yang, Q.; Hellinger, R.; Hermann, M. Activation of the calcium-sensing receptor by a subfraction of amino acids contained in thyroid drainage fluid. *ACS Pharmacol. Transl. Sci.* **2024**, *7*, 1937–1950. [CrossRef]
30. Mumpton, F.A. La roca magica: Uses of natural zeolites in agriculture and industry. *Proc. Natl. Acad. Sci. USA* **1999**, *96*, 3463–3470. [CrossRef]
31. Eroglu, N.; Emekci, M.; Athanassiou, C. Applications of natural zeolites on agriculture and food production. *J. Sci. Food Agric.* **2017**, *97*, 3487–3499. [CrossRef]
32. Tschegg, C.; Rice, A.H.N.; Grasemann, B.; Matiasek, E.; Kobulej, P.; Dzivák, M.; Berger, T. Petrogenesis of a large-scale miocene zeolite tuff in the Eastern Slovak Republic: The Nižný Hrabovec open-pit clinoptilolite mine. *Econ. Geol.* **2019**, *114*, 1177–1194. [CrossRef]
33. Tschegg, C.; Hou, Z.; Rice, A.H.N.; Fendrych, J.; Matiasek, E.; Berger, T.; Grasemann, B. Fault zone structures and strain localization in clinoptilolite-tuff (Nižný Hrabovec, Slovak Republic). *J. Struct. Geol.* **2020**, *138*, 104090. [CrossRef]
34. Samekova, K.; Firbas, C.; Irrgeher, J.; Opper, C.; Prohaska, T.; Retzmann, A.; Tschegg, C.; Meisslitzer, C.; Tchaikovsky, A.; Gouya, G.; et al. Concomitant oral intake of purified clinoptilolite-tuff (G-PUR) reduces enteral lead uptake in healthy humans. *Sci. Rep.* **2021**, *11*, 14796. [CrossRef] [PubMed]
35. Ranftler, C.; Nagl, D.; Sparer, A.; Röhrich, A.; Freissmuth, M.; El-Kasaby, A.; Nasrollahi Shirazi, S.; Koban, F.; Tschegg, C.; Nizet, S. Binding and neutralization of C. difficile toxins A and B by purified clinoptilolite-tuff. *PLoS ONE* **2021**, *16*, e0252211. [CrossRef]
36. Nizet, S.; Muñoz, E.; Fiebich, B.L.; Abuja, P.M.; Kashofer, K.; Zatloukal, K.; Tangermann, S.; Kenner, L.; Tschegg, C.; Nagl, D.; et al. Clinoptilolite in dextran sulphate sodium-induced murine colitis: Efficacy and safety of a microparticulate preparation. *Inflamm. Bowel Dis.* **2017**, *24*, 54–66. [CrossRef] [PubMed]
37. Yamaguchi, Y.; Yoshikawa, K. Cutaneous wound healing: An update. *J. Dermatol.* **2001**, *28*, 521–534. [CrossRef]
38. Singh, A.V.; Gemmati, D.; Kanase, A.; Pandey, I.; Misra, V.; Kishore, V.; Jahnke, T.; Bill, J. Nanobiomaterials for vascular biology and wound management: A review. *Veins Lymphat.* **2018**, *7*, 7196. [CrossRef]
39. Numata, Y.; Terui, T.; Okuyama, R.; Hirasawa, N.; Sugiura, Y.; Miyoshi, I.; Watanabe, T.; Kuramasu, A.; Tagami, H.; Ohtsu, H. The accelerating effect of histamine on the cutaneous wound-healing process through the action of basic fibroblast growth factor. *J. Investig. Dermatol.* **2006**, *126*, 1403–1409. [CrossRef] [PubMed]
40. Ashida, Y.; Denda, M.; Hirao, T. Histamine H1 and H2 receptor antagonists accelerate skin barrier repair and prevent epidermal hyperplasia induced by barrier disruption in a dry environment. *J. Investig. Dermatol.* **2001**, *116*, 261–265. [CrossRef]
41. Lim, H.K.; Rahim, A.B.; Leo, V.I.; Das, S.; Lim, T.C.; Uemura, T.; Igarashi, K.; Common, J.; Vardy, L.A. Polyamine regulator AMD1 promotes cell migration in epidermal wound healing. *J. Investig. Dermatol.* **2018**, *138*, 2653–2665. [CrossRef] [PubMed]
42. Ito, D.; Ito, H.; Ideta, T.; Kanbe, A.; Ninomiya, S.; Shimizu, M. Systemic and topical administration of spermidine accelerates skin wound healing. *Cell Commun. Signal.* **2021**, *19*, 36. [CrossRef]
43. Johnson, L.; Mulcahy, H.; Kanevets, U.; Shi, Y.; Lewenza, S. Surface-localized spermidine protects the Pseudomonas aeruginosa outer membrane from antibiotic treatment and oxidative stress. *J. Bacteriol.* **2012**, *194*, 813–826. [CrossRef]
44. Hasan, C.M.; Pottenger, S.; Green, A.E.; Cox, A.A.; White, J.S.; Jones, T.; Winstanley, C.; Kadioglu, A.; Wright, M.H.; Neill, D.R.; et al. Pseudomonas aeruginosa utilizes the host-derived polyamine spermidine to facilitate antimicrobial tolerance. *JCI Insight* **2022**, *7*, e158879. [CrossRef] [PubMed]
45. Cutting, K.F. Wound exudate: Composition and functions. *Br. J. Community Nurs.* **2003**, *8* (Suppl. S9), 4–9. [CrossRef]
46. Percival, S.L.; McCarty, S.; Hunt, J.A.; Woods, E.J. The effects of pH on wound healing, biofilms, and antimicrobial efficacy. *Wound Repair Regen.* **2014**, *22*, 174–186. [CrossRef] [PubMed]
47. Ono, S.; Imai, R.; Ida, Y.; Shibata, D.; Komiya, T.; Matsumura, H. Increased wound pH as an indicator of local wound infection in second degree burns. *Burns* **2015**, *41*, 820–824. [CrossRef]
48. Shukla, V.K.; Shukla, D.; Tiwary, S.K.; Agrawal, S.; Rastogi, A. Evaluation of pH measurement as a method of wound assessment. *J. Wound Care* **2007**, *16*, 291–2944. [CrossRef] [PubMed]
49. Alavi, A.; Farzanfar, D.; Lee, R.K.; Almutairi, D. The contribution of malodour in quality of life of patients with hidradenitis suppurativa. *J. Cutan. Med. Surg.* **2018**, *22*, 166–174. [CrossRef]
50. Hubner, P.; Donati, N.; Quines, L.K.M.; Tessaro, I.C.; Marcilio, N.R. Gelatin-based films containing clinoptilolite-Ag for application as wound dressing. *Mater. Sci. Eng. C Mater. Biol. Appl.* **2020**, *107*, 110215. [CrossRef] [PubMed]